Self-referenced photonic molecule bio(chemical)sensor

Svetlana V. Boriskina* and Luca Dal Negro

Department of Electrical and Computer Engineering & Photonics Center, Boston University, Boston, Massachusetts 02215, USA
**Corresponding author: sboriskina@gmail.com*

Received April 23, 2010; accepted June 4, 2010;
posted July 2, 2010 (Doc. ID 127502); published July 15, 2010

We report a new type of optical biosensor capable of differentiating between bulk and surface perturbations of the ambient refractive index as well as between specific and nonspecific binding of molecules on the sensor surface. The proposed detection scheme is based on tracking the shifts of hybridized bonding and antibonding optical modes in coupled optical microcavities (photonic molecules). We demonstrate that by using two measurements of spectral shifts it is possible to discriminate between surface and volume index perturbation, to detect specific target molecules in a complex environment and to estimate the thickness of thin layers of adsorbed molecules.

OCIS codes: 280.4788, 170.4580, 230.5750, 230.4555, 300.6490, 130.7408.

Optical microcavities supporting high-Q whispering-gallery mode (WGM) resonances have long been established as ultrasensitive on-chip platforms for real-time label-free bio(chemical) sensing [1,2]. Spectral positions of the WGMs are very sensitive to changes in the bulk refractive index of the ambient medium and can be used for detecting target molecules such as glucose [3], NaCl [4], and D_2O [2] in a solution and measuring their concentration. Binding of molecules on the microcavity surface changes its refractive index and results in shifting of the WGM resonances, providing another sensing modality of microcavity sensors [4–6]. Targeted detection can be achieved by microcavity surface modification with functional groups that provide binding with specific receptors [7,8]. Although bulk index changes and adsorption of molecules on the microcavity surface cause different spectral shifts of the WGM resonant peaks [4,5,8], discrimination between the two scenarios requires an *a priori* knowledge of the molecules present in the solution and may not be possible in a complex multitarget environment. Furthermore, indiscriminate adsorption of nonspecific molecules can generate the same signal as binding of a specific target, making it difficult or even impossible to differentiate between the two events. Here, we propose a self-referenced sensor based on coupled microcavities ("photonic molecules" (PMs) [9]) that is capable of discriminating between bulk index changes and specific/nonspecific surface binding events and thus provides a significant advantage over conventional single-cavity sensors for drug discovery and point-of-care testing applications.

If two microcavities are located close to each other, destructive/constructive interference of their WGM evanescent fields results in the formation of bonding (B) and antibonding (AB) PM supermodes with either even (++) or odd (+−) parity of their optical fields with respect to the PM axis of symmetry (see [9] and references therein). Such modes hybridization is a direct analogy to the formation of bonding and antibonding molecular orbitals in diatomic chemical molecules. We consider a PM composed of two silica microspheres coupled via a subwavelength gap; however, the proposed devices can be based on other types of PMs, including coupled microdisks, microtoroids, and defect nanocavities in photonic crystals. Traditionally, excitation of WGMs in optical microcavities has been achieved by coupling them to optical fibers or waveguides [3,7]; however, recent experiments with active microcavities [5,6] paved the way for remote excitation/detection schemes that make possible simultaneous excitation and monitoring of multiple WGMs within a certain frequency band. The proposed PM sensors can be used in both types of excitation/detection schemes; here we consider the case of remote excitation with a linearly polarized plane wave propagating along the PM major axis. All the numerical results presented in this Letter have been obtained by using the generalized multiparticle Mie theory [10].

The WGM spectra of a single 10 μm diameter silica microsphere ($n_m = 1.45$) and two coupled identical microspheres in the free space are shown in Figs. 1(a) and 1(b), where we plot the total scattering efficiency [10] as a function of wavelength. The inset in Fig. 1(a) shows the single-sphere scattering efficiency within the frequency range around the resonant peak corresponding to the excitation of the fundamental $WG_{37,1}$ mode [with one radial and 37 azimuthal field variations; see Fig. 1(c)].

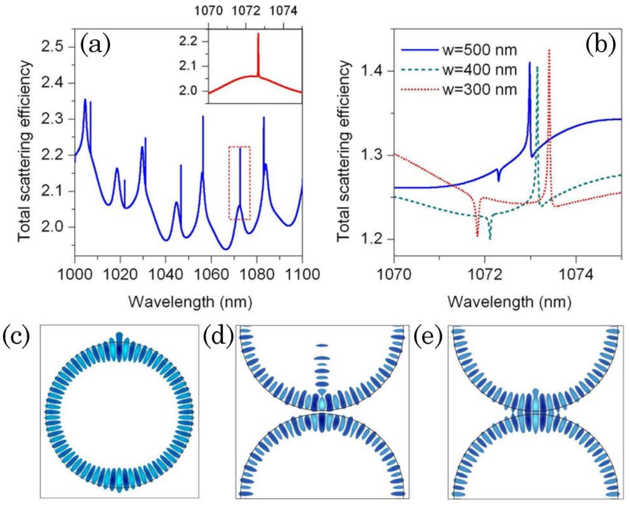

Fig. 1. (Color online) WG modes resonant peaks in the plane-wave scattering spectra of (a) a single silica 10 μm diameter microsphere and (b) double-microsphere PMs with varying air-gap widths w. Electric field distributions of (c) the fundamental $WG_{37,1}$ mode in the microsphere and (d), (e) the hybridized bonding and antibonding supermodes in the PM with $w = 300$ nm.

Although the Q-factor and sensitivity of a WGM depends on its radial and azimuthal mode numbers [9,11,12], the proposed concept of the self-referenced sensing is general and does not depend on the choice of the mode. The PM optical spectrum has two narrow features within the same frequency range [see Fig. 1(b)], which correspond to B and AB PM supermodes with the intensity patterns shown in Figs. 1(d) and 1(e). B (AB) supermode resonance appears as peak (dip) in the PM spectrum, which reflects a constructive (destructive) interference of interacting fields. As illustrated in Fig. 1(b), the spectral positions of these features depend on the width of the airgap between the microspheres, and their separation increases with the increase of the coupling strength. It should be noted that optical coupling between WGMs of two microcavities results in a complex picture of modes hybridization [9]; however, only two sharp spectral features corresponding to the fundamental B and AB supermodes are usually pronounced in the PM scattering spectrum.

We will now compare the spectral responses of the single microsphere and the PM to a bulk refractive index change and an adsorption of a thin layer of molecules on the sphere surface. Since many biomolecules of interest (such as small proteins) have dielectric constants very close to that of silica, the effect of binding a compact molecule layer of thickness d is modeled by increasing the radius of the sphere by d [1]. The scattering spectra of the single sphere for varied bulk index values and varied thicknesses of the index-matched layers are shown in Figs. 2(a) and 2(b), respectively. The resonant wavelength of the single-sphere WGM is plotted as a function of the index change $\Delta n = n_a - n_a^0$ ($n_a^0 = 1$) and the layer thickness d in Figs. 2(c) and 2(d), respectively. Comparison of Figs. 2(c) and 2(d) reveals higher sensitivity of the WGM resonant wavelength to the surface binding events (see also [1,4,5,8]). However, a detection of a wavelength shift $\Delta\lambda$ can be attributed to either a bulk index change or a surface binding event. Furthermore, both events can occur simultaneously, or an indiscriminate surface adsorption of other nonspecific molecular targets can take place. It is possible to distinguish between bulk and surface changes by measuring the spectral shifts of two WGMs spectrally separated from each other [4], which, however, requires exciting the microcavity with two very different wavelengths and does not allow for discriminating between specific and not-specific binding events. Using two coupled microcavities provides a self-referencing mechanism that makes it possible to distinguish between various bulk and surface index variations. If only one of the two microcavities is functionalized for binding a specific molecular target, a specific binding event will change the radius of one microcavity, while an indiscriminate binding will result in the increase of the radii of both microcavities. As A and AB supermodes feature markedly different intensity distributions in the PM gap region [Figs. 1(d) and 1(e)], they experience different shifts in response to bulk and surface index perturbations.

This concept is illustrated in Fig. 3. The scattering efficiency spectra for three different values of the bulk ambient refractive index and for three values of the thickness of the index-matched layer adsorbed on the surface of one microcavity are presented in Figs. 3(a) and 3(b), respectively. Clearly, the two resonant features experience different spectral shifts in response to localized and homogeneous index perturbations. The shifts of the resonant wavelengths of B and AB PM supermodes are plotted in Fig. 3(c) as a function of the bulk ambient index and compared to the corresponding shifts caused

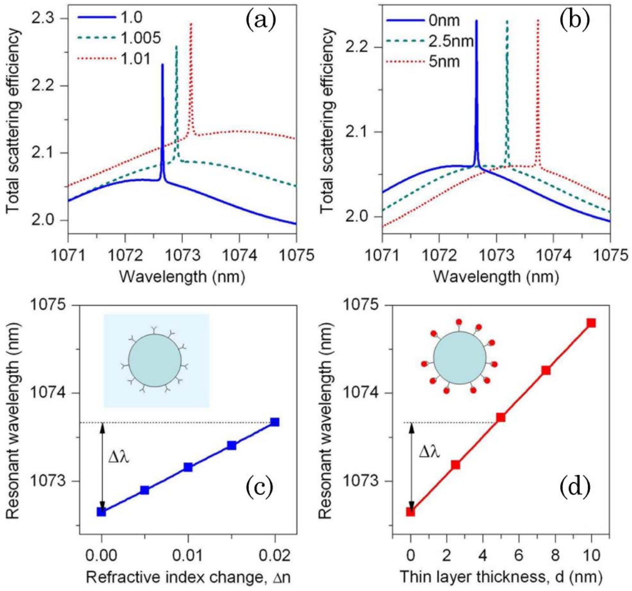

Fig. 2. (Color online) Shift of the resonant peak in the microsphere spectrum caused by (a) the change of the bulk ambient refractive index and (b) the absorption of a thin index-matched dielectric layer of varied thickness. The labels correspond to (a) the ambient index value n_a and (b) the layer thickness d. WG mode resonant wavelength as a function of (c) the ambient refractive index and (d) the thin layer thickness.

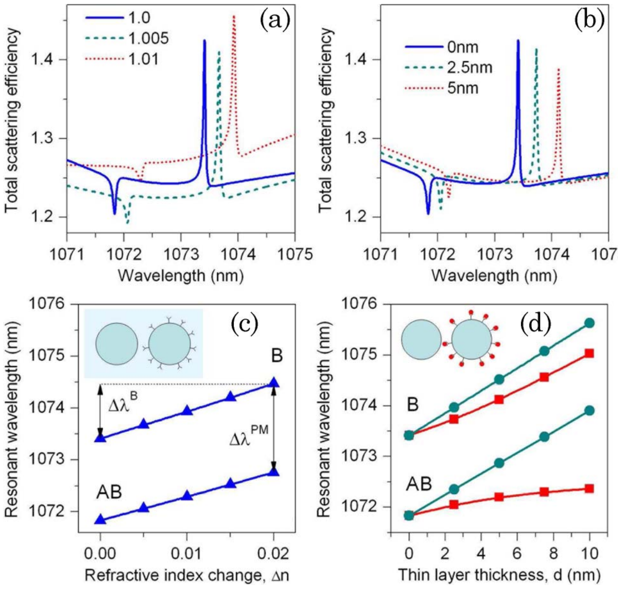

Fig. 3. (Color online) Shifts of the resonant peaks in the PM spectrum caused by (a) the change of the bulk ambient refractive index and (b) the absorption of a thin index-matched dielectric layer of varied thickness on the surface of one of the microspheres (squares) and of both microspheres (circles). WG supermodes resonant wavelengths as a function of (c) the ambient refractive index and (d) the thin layer thickness.

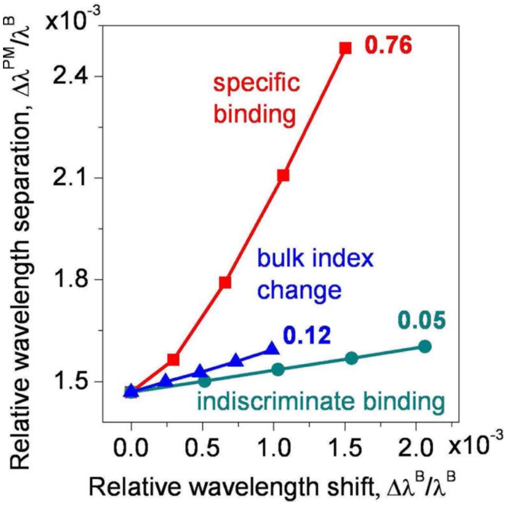

Fig. 4. (Color online) Comparison of the changes in the separation between the resonant wavelengths of the B and AB PM supermodes caused by the ambient refractive index variation (triangles), by the specific binding of molecules to the surface of one of the microspheres (squares), and by a nonspecific binding to both the microspheres (circles). The numbers represent the slopes of the corresponding curves.

by specific (squares) and nonspecific (circles) surface binding shown in Fig. 3(d). As indicated in Fig. 3(c), there are two parameters that can be monitored simultaneously: (1) the spectral shift of B resonance and (2) the spectral separation between B and AB resonances. These two measurements can be used to detect perturbations in the ambient medium, to distinguish between different types of perturbations, and to measure the thickness of thin layers of adsorbed molecules.

The results are summarized in Fig. 4. Here, we plot the relative spectral separation between B and AB resonances $\Delta\lambda^{\mathrm{PM}}/\lambda^{\mathrm{B}}$ versus the relative spectral shift of the bonding supermode resonance $\Delta\lambda^{\mathrm{B}}/\lambda^{\mathrm{B}}$. It can be clearly seen that the three curves corresponding to different types of refractive index perturbation have different slopes (shown as labels next to the corresponding curves). Therefore, by plotting the result of two measurements of the relative spectral shift and mode separation and comparing it to the calibration curves shown in Fig. 4 it is possible to attribute the observed mode shifts to a specific type of index perturbation and to estimate the thickness of the adsorbed molecular layer. Furthermore, as the slope of the curve corresponding to the specific binding is much larger than those corresponding to the bulk changes and indiscriminate adsorption, specific target molecules can be detected even in complex environments where bulk changes and indiscriminate adsorption of other materials can occur.

Summarizing, we proposed and demonstrated a new type of optical sensor that exploits unique spectral properties of hybridized optical supermodes in photonic molecules. PMs can be composed of microcavities of either equal or different sizes, which eases fabrication tolerances of the proposed devices [12]. Microcavities can also be made of different materials, which can have affinity for binding of a specific target material, thus eliminating the need for the chemical functionalization step. Arrays of PM-based sensors each functionalized for a specific target molecule can also be used for multiplexed sensing [7]. We believe the proposed self-referenced detection scheme may enable a new class of platforms for label-free real-time bio(chemical) sensing and thin-film growth monitoring.

The authors thank Dr. Frank Vollmer for useful discussions.

References

1. F. Vollmer and S. Arnold, Nature Meth. **5**, 591 (2008).
2. A. M. Armani and K. J. Vahala, Opt. Lett. **31**, 1896 (2006).
3. C. Y. Chao and L. J. Guo, Appl. Phys. Lett. **83**, 1527 (2003).
4. M. Noto, F. Vollmer, D. Keng, I. Teraoka, and S. Arnold, Opt. Lett. **30**, 510 (2005).
5. H. Beier, G. Coté, and K. Meissner, Ann. Biomed. Eng. **37**, 1974 (2009).
6. A. Francois and M. Himmelhaus, Appl. Phys. Lett. **94**, 031101 (2009).
7. F. Vollmer, S. Arnold, D. Braun, I. Teraoka, and A. Libchaber, Biophys. J. **85**, 1974 (2003).
8. A. Yalcin, K. C. Popat, J. C. Aldridge, T. A. Desai, J. Hryniewicz, N. Chbouki, B. E. Little, O. King, V. Van, S. Chu, D. Gill, M. Anthes-Washburn, S. M. Ünlü, and B. Goldberg, IEEE J. Sel. Top. Quantum Electron. **12**, 148 (2006).
9. S. V. Boriskina, in *Photonic Microresonator Research and Applications*, I. Chremmos, O. Schwelb, and N. Uzunoglu, eds. (Springer, Dordrecht, 2010).
10. D. W. Mackowski, Proc. R. Soc. Edinb., A **433**, 599 (1991).
11. S. V. Boriskina, J. Opt. Soc. Am. B **23**, 1565 (2006).
12. S. V. Boriskina, Opt. Lett. **32**, 1557 (2007).